**Supporting Information for**

**Title**: Potent PBS/Polysorbate-Soluble Transplatin-Derived Porphyrin-Based Photosensitizers for Photodynamic Therapy

**Authors:**

Lukas Schneider,[1] Martina Kalt,[1] Michele Larocca,[1] Vipin Babu,[1] Bernhard Spingler[1*]

**Affiliations:**

[1]Department of Chemistry, University of Zurich, CH-8057 Zurich, Switzerland.

[1] To whom correspondence should be addressed. E-mail: spingler@chem.uzh.ch

## Content

## 1. Synthetic Procedures to Yield Non-Platinated Porphyrins

### 1.1. $H_2$3PyP (5,10,15,20-tetra(3'-pyridyl)porphyrin)[1]

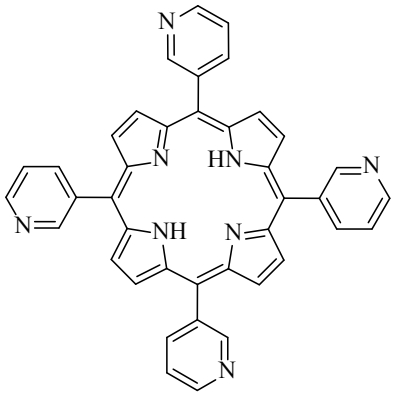

3-Pyridinecarboxaldehyde (4.40 mL, 46.7 mmol) was dissolved in 130 mL of propionic acid at 23 °C while stirring, before pyrrole (3.30 mL, 46.7 mmol) was added and the mixture was refluxed at 145 °C under an atmosphere of air for 1 h. Afterwards, the mixture was cooled for 30 minutes using an ice-water bath. The excess of propionic acid was removed *in vacuo*, before 150 mL of a 10% DMF solution in EtOH were added. After leaving the resulting suspension at 23 °C for 4 h, it was filtered and the resulting purple solid was collected by washing the filter cake with EtOH, acetone and $CHCl_3$ to leave a grey solid remaining in the frit, which was discarded. The combined organic fractions were combined, dried *in vacuo* and the purification procedure including the addition of the 10% DMF solution in EtOH was repeated. **$H_2$3PyP** was obtained as a violet solid in a yield of 12% (950.0 mg, 1.401 mmol).

**Analytical Data:** ($C_{40}H_{26}N_8$), Mol. Wt.: 618.70 g/mol. UV-Vis (DMF): (nm, log(ε)) $\lambda_{max}$ 417.1 (6.9, B-band), $\lambda_{max}$ 513.3 (4.3, Q-band 1), $\lambda_{max}$ 547.2 (3.9, Q-band 2), $\lambda_{max}$ 589.0 (3.8, Q-band 3), $\lambda_{max}$ 644.8 (3.6, Q-band 4). IR (FT-IR): ($cm^{-1}$) 1565, 1467, 1406, 1353, 1228, 1181, 1027, 966, 791, 710, 626. $^1$H-NMR (400 MHz, $CDCl_3$): $\delta$ (ppm) 9.51 (*s*, 4 H, 2′-H), 9.12 (*dd*, 4 H, $J_{ab}$ = 5.0 Hz, $J_{ac}$ = 1.3 Hz, 6′-H), 8.91 (*s*, 8 H, β-H), 8.57 (*d*, 4 H, *J* = 7.6 Hz, 4′-H), 7.82 (*dd*, 4 H, $J_{ab}$ = 7.4 Hz, $J_{ac}$ = 5.0 Hz, 5′-H), -2.78 (*s*, 2 H, N-H). HR-(+)-ESI-MS: m/z = 619.23531 $[M + H]^+$.

**1.2.** **Zn3PyP** (5,10,15,20-tetra(3'-pyridyl)-zinc(II)porphyrin)[2]

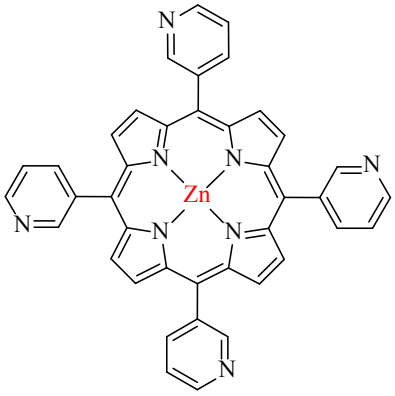


**$H_2$3PyP** (50.0 mg, 0.081 mmol) was suspended in 8 mL of a 1:1 DMF/water mixture before $ZnCl_2 \cdot (H_2O)_2$ (56.8 mg, 0.320 mmol) was added and the mixture stirred at 120 °C for 48 h. After that, the mixture was cooled down to room temperature and poured into ice-cold water. The resulting solid was filtered and further washed with water (10 mL), MeOH (10 mL) and diethyl ether (10 mL) before it was resuspended in MeCN (30 mL) and heated for 10 min at 55 °C. The mixture was left at 23 °C for 12 h and the resulting solid was filtered and dried *in vacuo*. The latter procedure was repeated replacing MeCN with water with a precipitation time of 3 h. The obtained solid was filtrated and dried *in vacuo*. **Zn3PyP** was obtained as a violet solid in a yield of 73% (40.0 mg, 0.059 mmol).

**Analytical Data:** ($C_{40}H_{24}N_8Zn$), Mol. Wt.: 682.07 g/mol. UV-Vis (DMF): (nm, log(ε)) $\lambda_{max}$ 425.0 (6.8, B-band), $\lambda_{max}$ 404.0 (4.2, Q-band 1), $\lambda_{max}$ 559.4 (3.8, Q-band 2), $\lambda_{max}$ 597.50 (3.7 Q-band 3). IR (FT-IR): ($cm^{-1}$) 1567, 1520, 1495, 1470, 1407, 1343, 1261, 1204, 1183, 1030, 1106, 1075, 993, 933, 886, 839, 743, 709, 692, 632. $^1$H-NMR (400 MHz, $CDCl_3$/MeOH-$d_4$ = 3:2): $\delta$ (ppm) 9.04 (*bs*, 4 H, 2′-H), 8.76 (*s*, 4 H, 6′-H), 8.70 (*bs*, 8 H, β-H), 8.56 (*bs*, 4 H, 4′-H), 7.77 (*bs*, 4 H, 5′-H). HR-(+)-ESI-MS: m/z = 681.14822 $[M + H]^+$.

## 2. HR-(+)-ESI-MS Spectra of cPt-$H_2$3PyP, tPt-$H_2$3PyP, cPt-Zn3PyP and tPt-Zn3PyP

### cPt-$H_2$3PyP

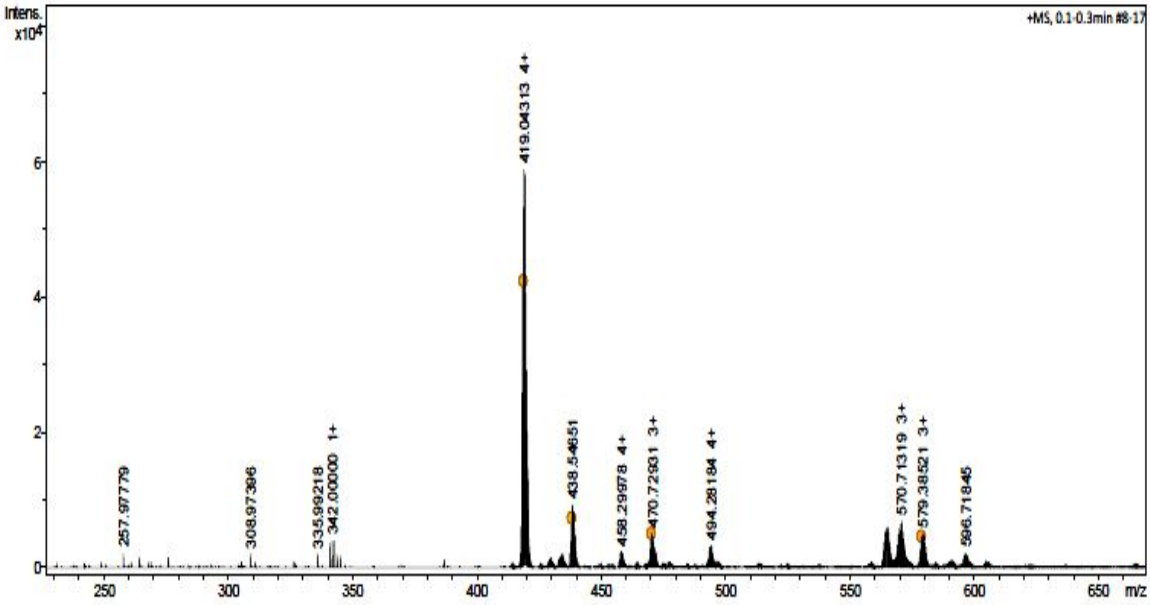


**Figure S1**. HR-(+)-ESI-MS spectrum of **cPt-$H_2$3PyP**.

### tPt-$H_2$3PyP

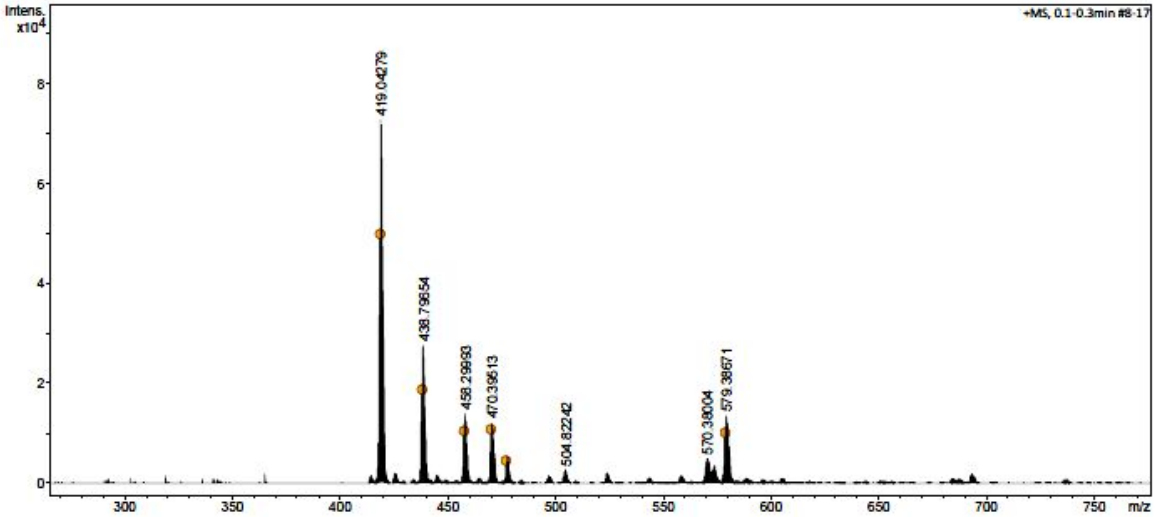


**Figure S2**. HR-(+)-ESI-MS spectrum of **tPt-$H_2$3PyP**.

**cPt-Zn3PyP**

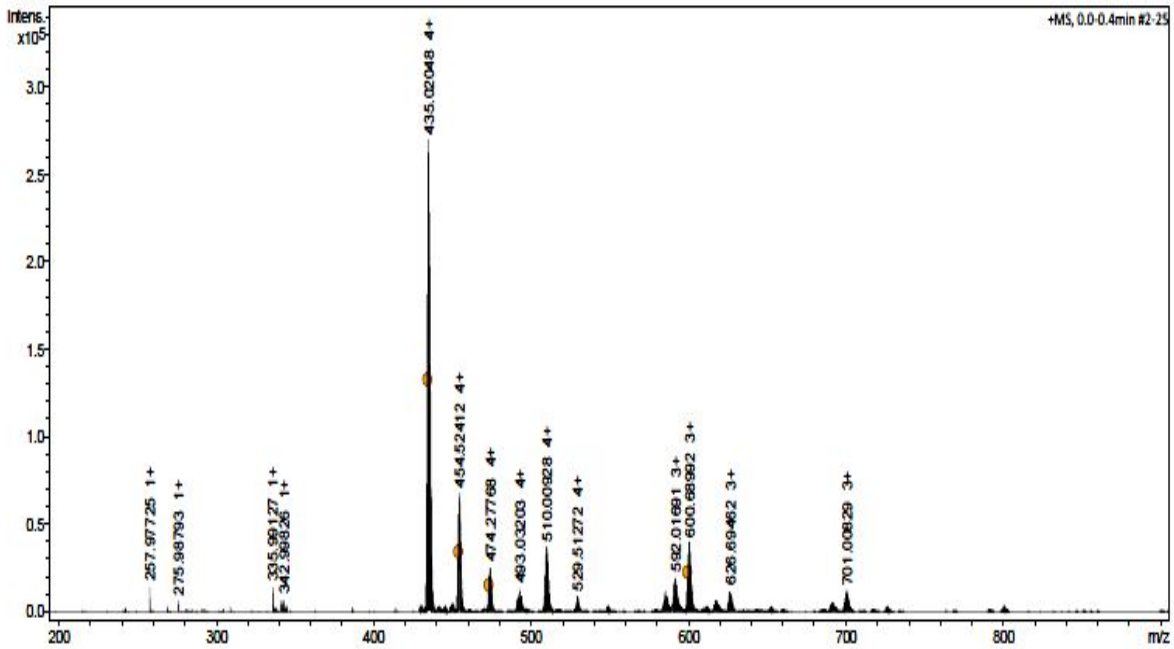


**Figure S3**. HR-(+)-ESI-MS spectrum of **cPt-Zn3PyP**.

**tPt-Zn3PyP**

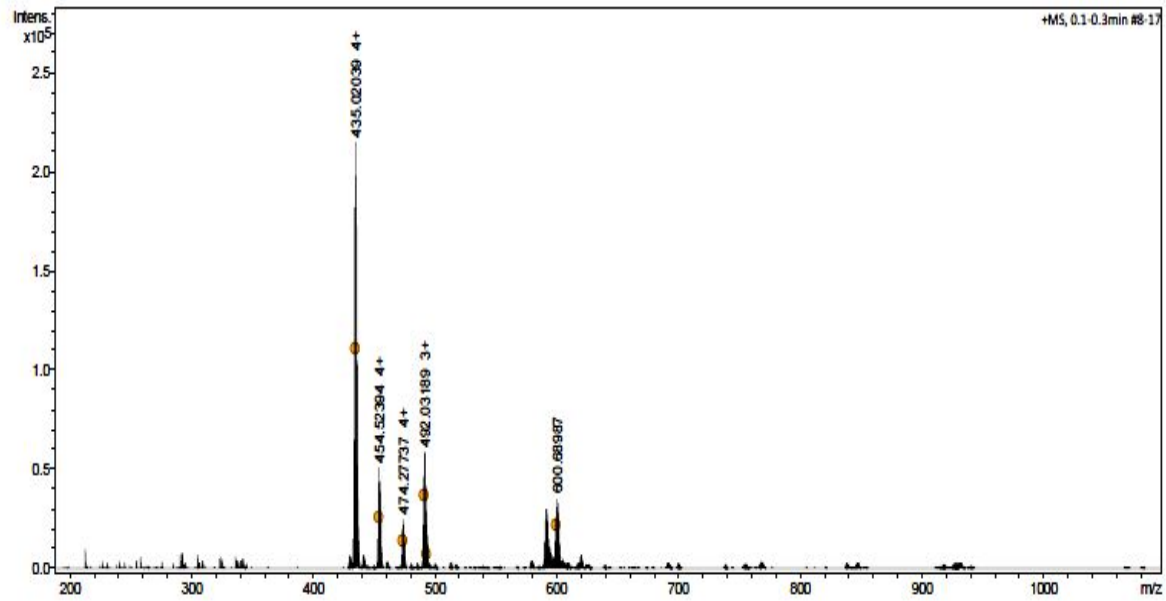


**Figure S4**. HR-(+)-ESI-MS spectrum of **tPt-Zn3PyP**.

## 3. $^{195}$Pt-NMR Spectra of cPt-$H_2$3PyP, tPt-$H_2$3PyP, cPt-Zn3PyP and tPt-Zn3PyP

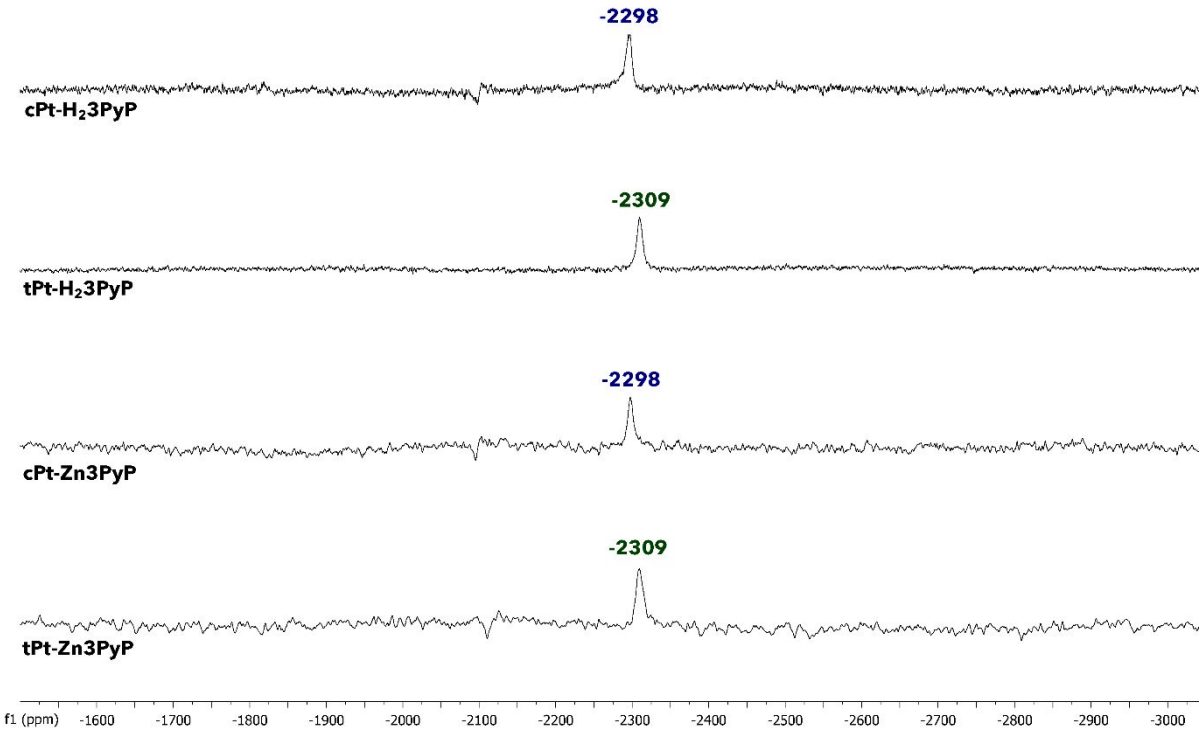


**Figure S5**. $^{195}$Pt-NMR spectra of **cPt-$H_2$3PyP**, **tPt-$H_2$3PyP**, **cPt-Zn3PyP** and **tPt-Zn3PyP** measured in DMF-$d_7$.

## 4. $^1$H-NMR Spectra of cPt-$H_2$3PyP, tPt-$H_2$3PyP, cPt-Zn3PyP and tPt-Zn3PyP

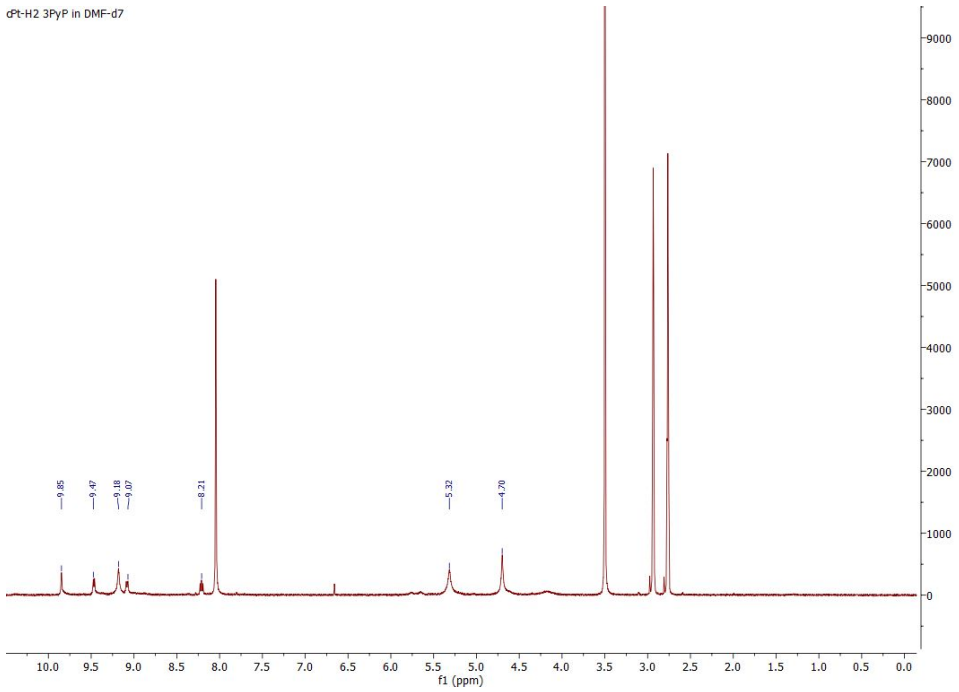


**Figure S6**. $^1$H-NMR spectrum of **cPt-$H_2$3PyP** measured in DMF-$d_7$.

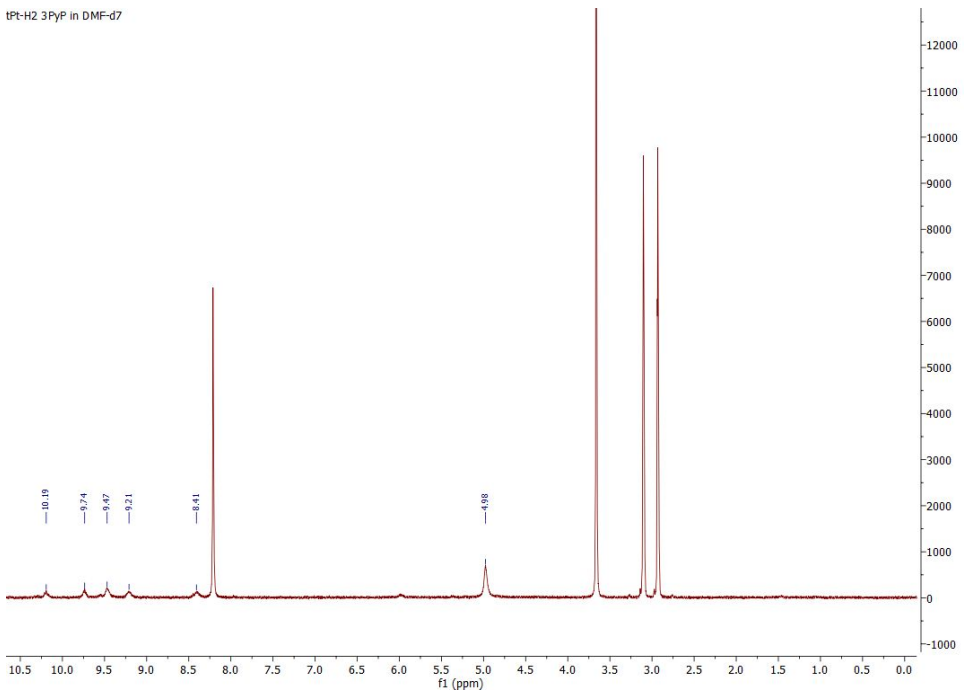


**Figure S7**. $^1$H-NMR spectrum of **tPt-$H_2$3PyP** measured in DMF-$d_7$.

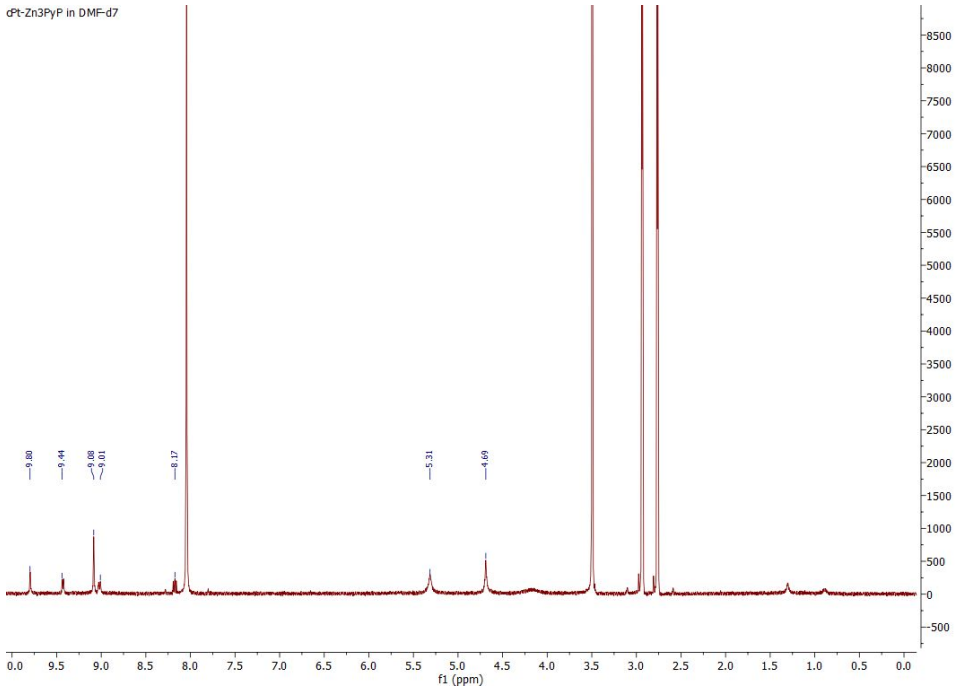


**Figure S8**. $^{1}$H-NMR spectrum of **cPt-Zn3PyP** measured in DMF-$d_7$.

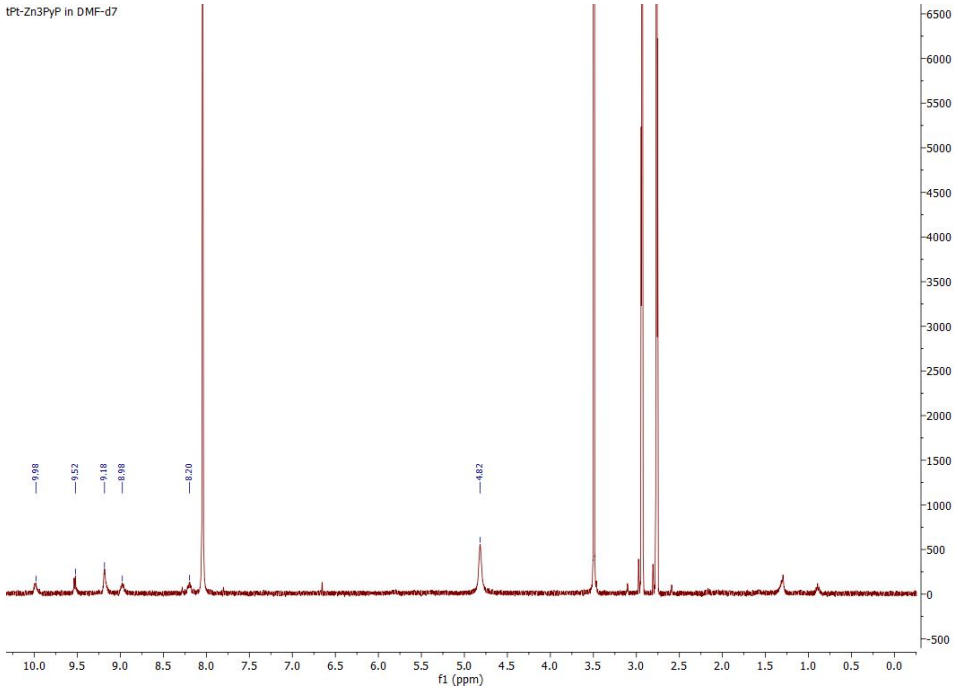


**Figure S9**. $^{1}$H-NMR spectrum of **tPt-Zn3PyP** measured in DMF-$d_7$.

## 5. $^{13}$C-NMR Spectra of cPt-$H_2$3PyP, tPt-$H_2$3PyP, cPt-Zn3PyP and tPt-Zn3PyP

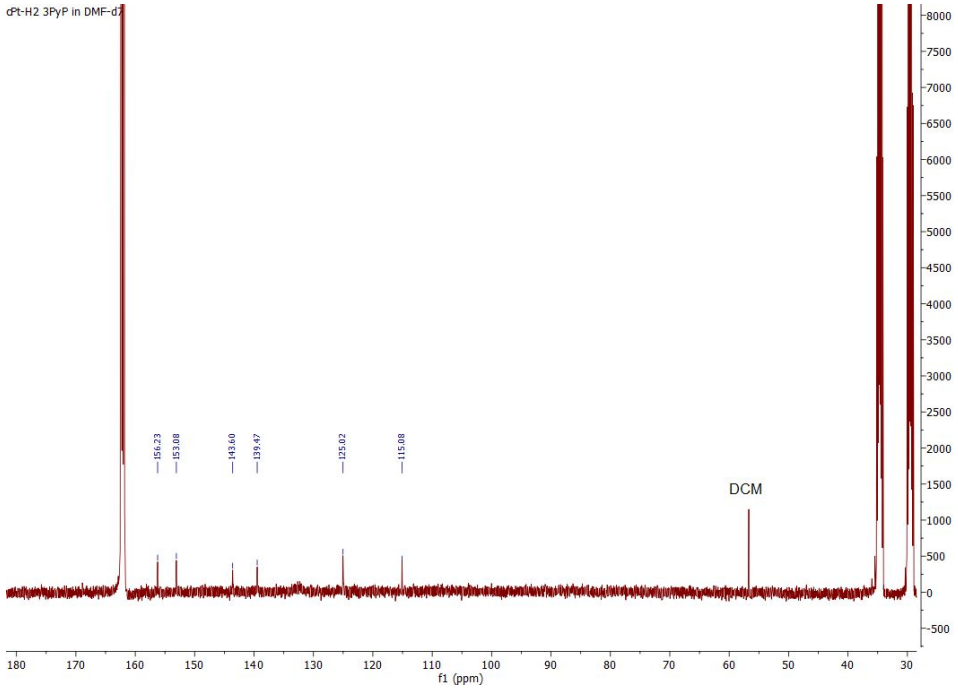


**Figure S10**. $^{13}$C-NMR spectrum of **cPt-$H_2$3PyP** measured in DMF-$d_7$.

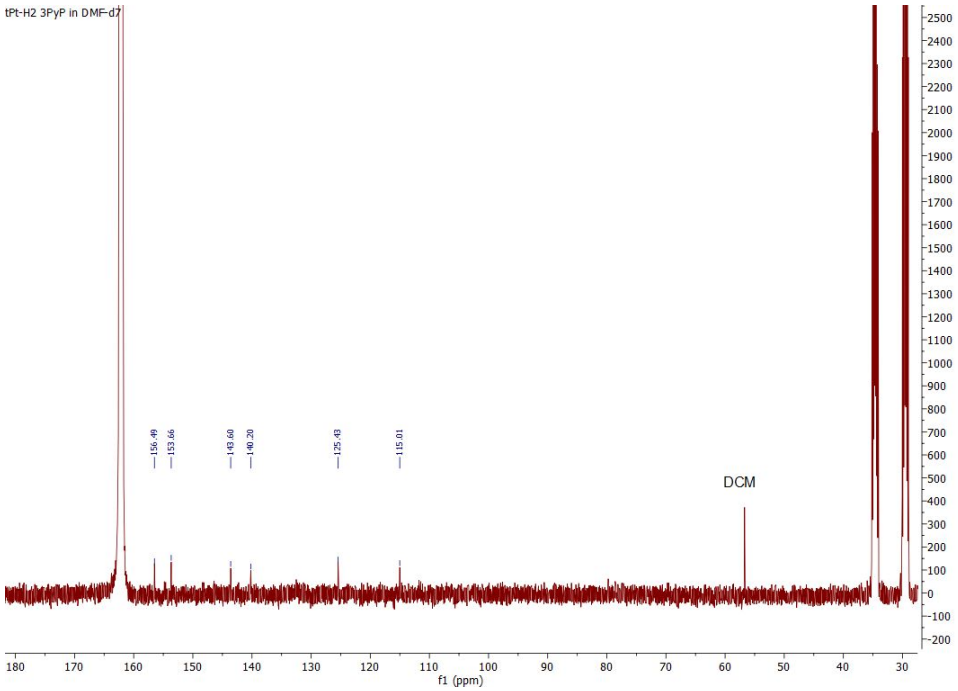


**Figure S11**. $^{13}$C-NMR spectrum of **tPt-$H_2$3PyP** measured in DMF-$d_7$.

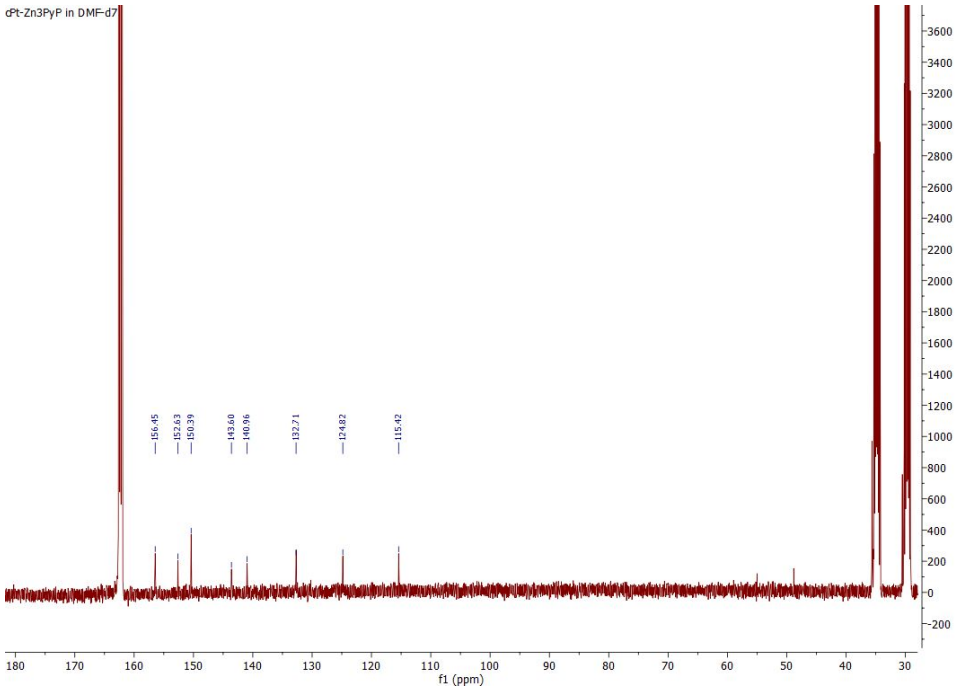


**Figure S12**. $^{13}$C-NMR spectrum of **cPt-Zn3PyP** measured in DMF-$d_7$.

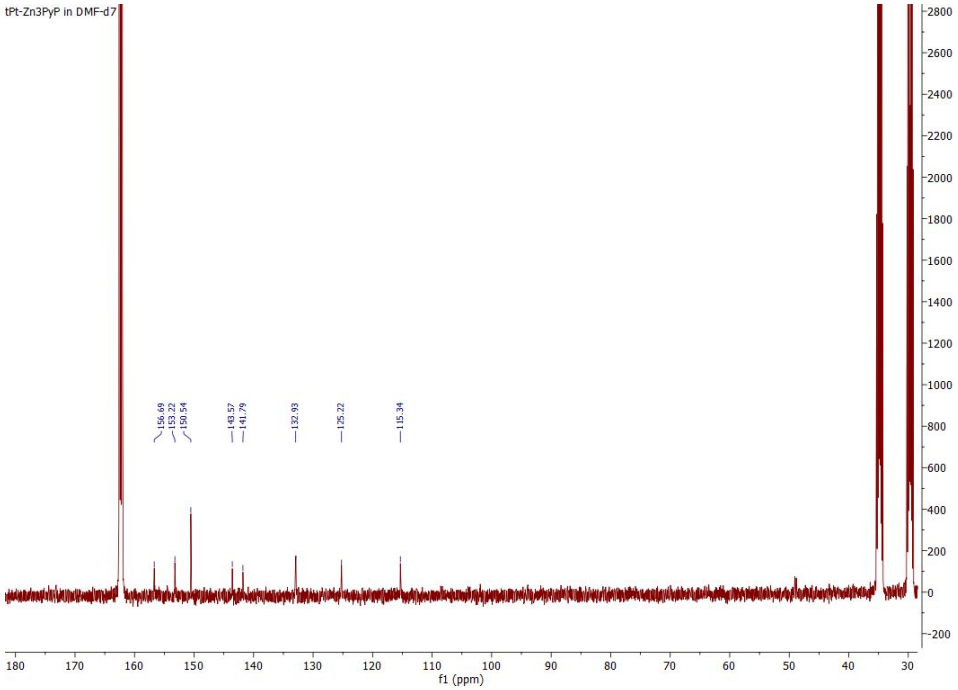


**Figure S13**. $^{13}$C-NMR spectrum of **tPt-Zn3PyP** measured in DMF-$d_7$.

## 6. FTIR Spectra of cPt-$H_2$3PyP, tPt-$H_2$3PyP, cPt-Zn3PyP and tPt-Zn3PyP

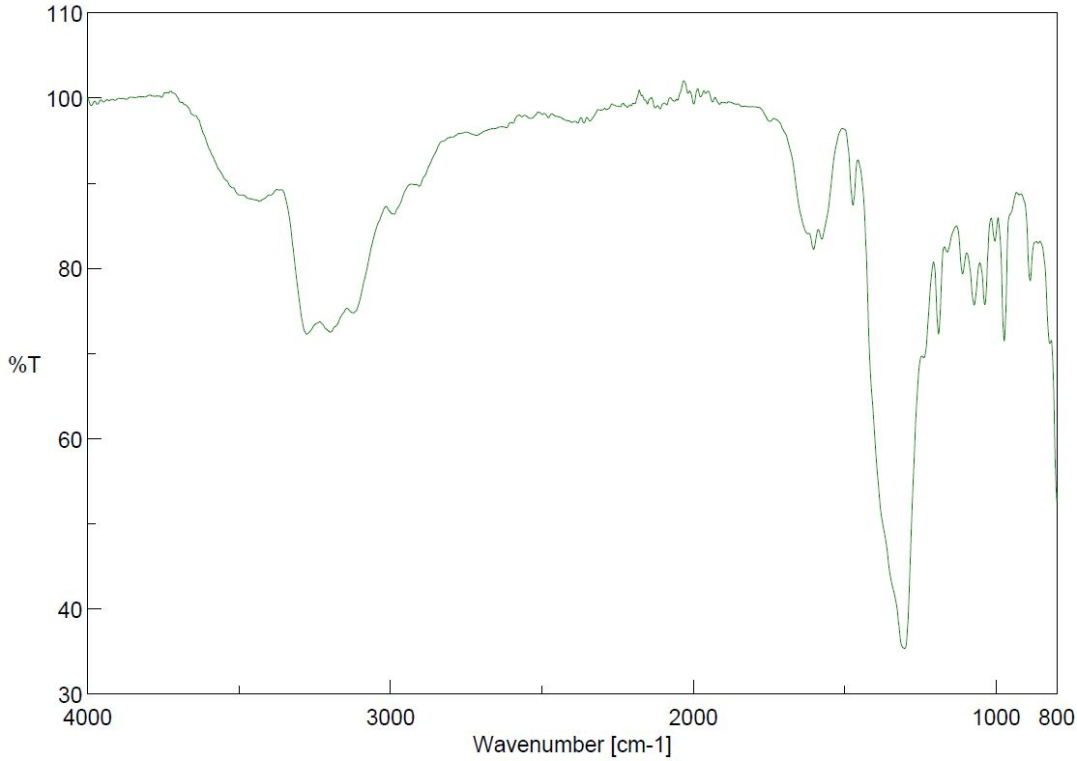


**Figure S14**. FTIR spectrum of **cPt-$H_2$3PyP**.

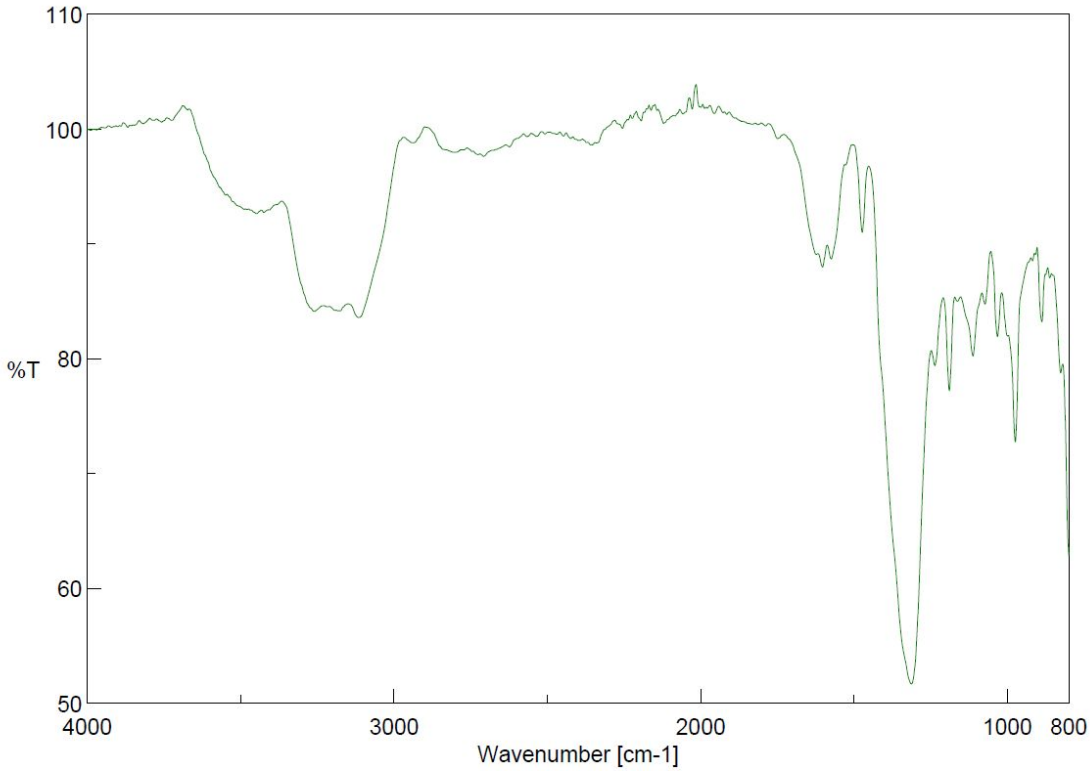


**Figure S15**. FTIR spectrum of **tPt-$H_2$3PyP**.

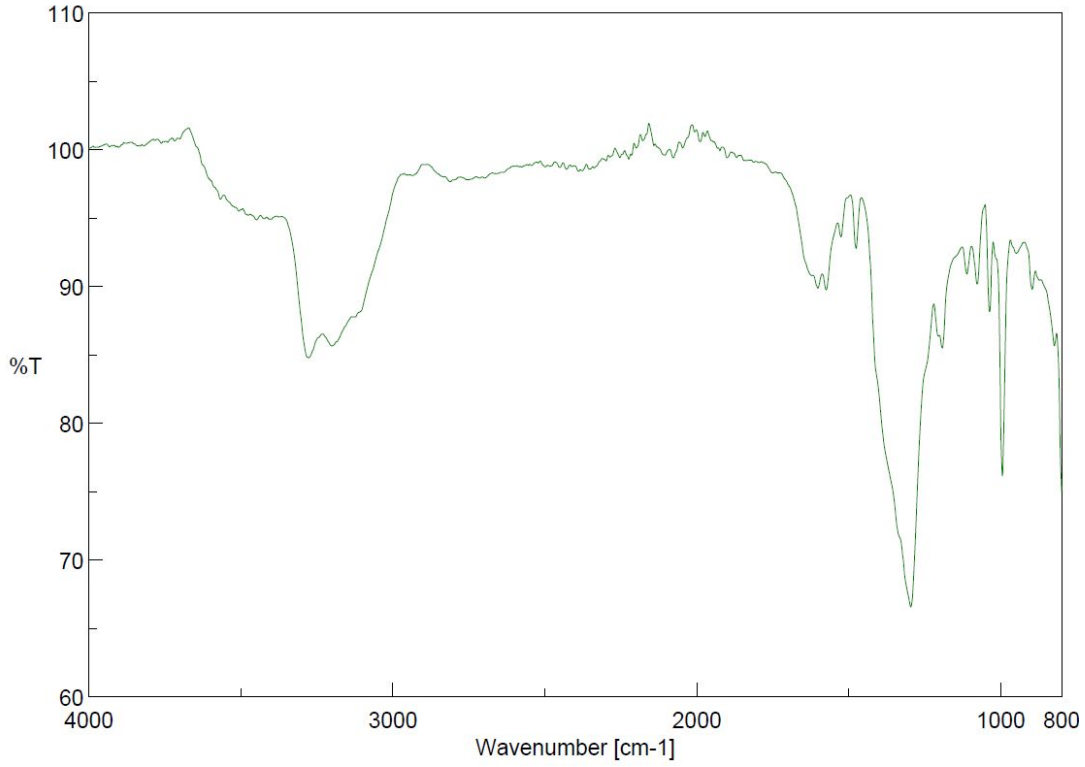


**Figure S16**. FTIR spectrum of **cPt-Zn3PyP**.

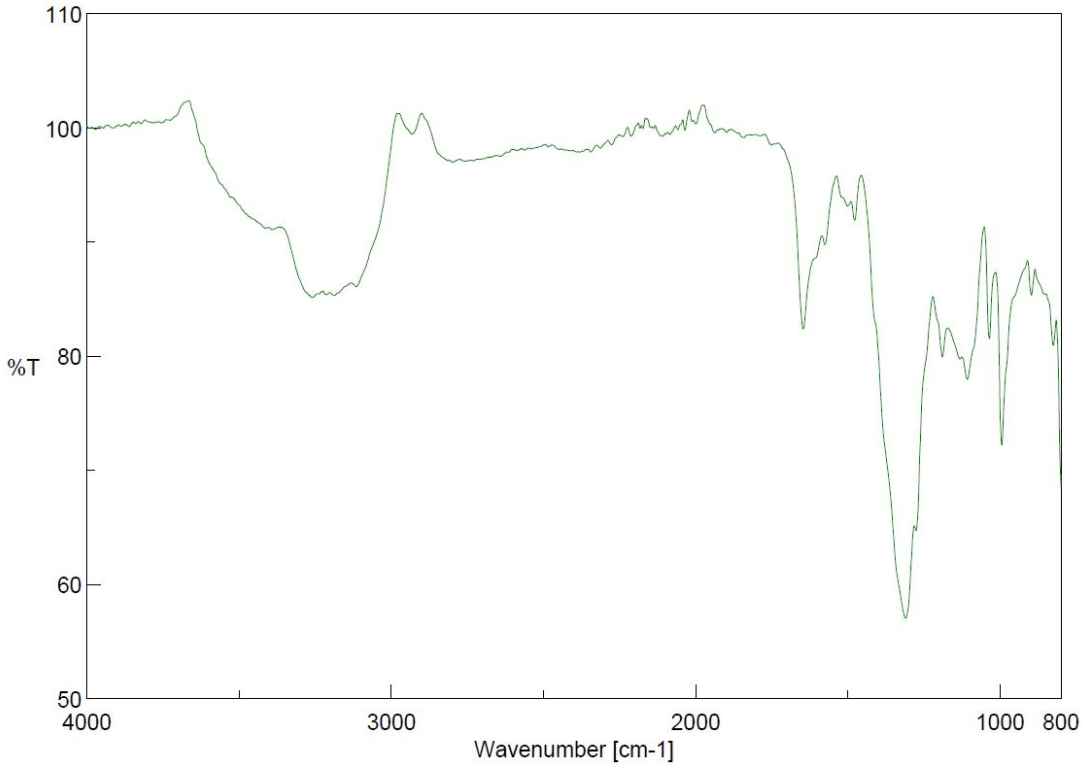


**Figure S17**. FTIR spectrum of **tPt-Zn3PyP**.

## 7. Determination of the Singlet Oxygen Quantum Yields

The singlet oxygen quantum yields ($\Phi_\Delta$) of **cPt-H$_2$3PyP**, **tPt-H$_2$3PyP**, **cPt-Zn3PyP** and **cPt-Zn3PyP** were determined analogously to a method reported by our group.[3] The PSs were dissolved in $D_2O$ and the solutions were placed in a glass cuvette (114F-10-40, 10 mm × 4 mm dimensions, *Hellma Analytics*, Germany). Three different concentrations were prepared for each PS, while the maximum absorption intensity of the highest concentrated sample did not exceed 1.0, with the cuvette oriented in a way that the light path equals to 10 mm. The cuvettes containing solutions of the same concentration as used for the corresponding UV-Vis spectroscopy measurements were placed in a CUV-UV/VIS-TC-ABS temperature-controlled Qpod sample compartment (*Avantes*, The Netherlands) and cooled to 20 °C; temperature control was performed with the use of a TC-125 controller (*Quantum Northwest*, USA) and Q-Blue software. Emission spectroscopy was conducted in a custom-built setup[3], that is based on the setup described by Bonnet and co-workers.[4] Excitation was performed using a high-power-LED 420 nm light source (**Figure S18**, FC5-LED-WL, *Prizmatix Ltd.*, Israel).

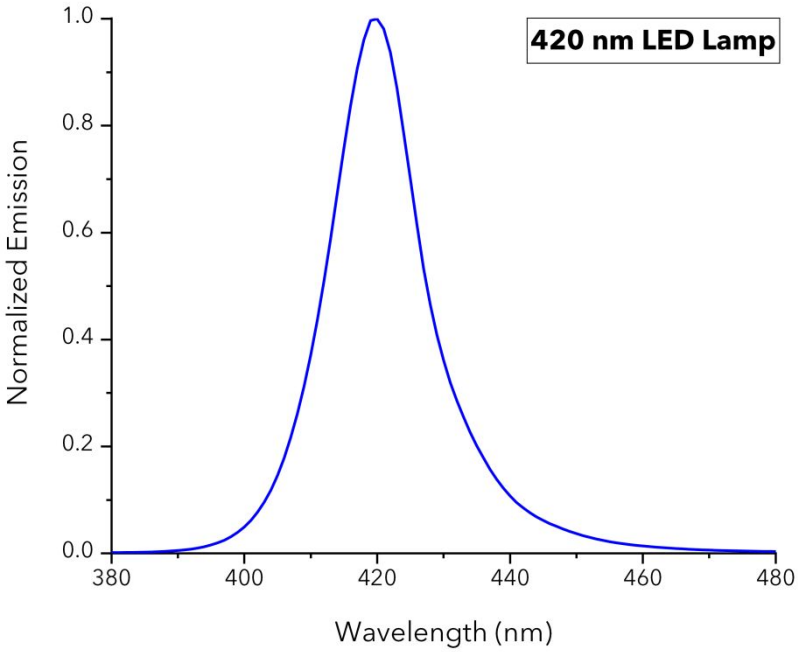


**Figure S18**. Normalized emission spectrum of the FC5-LED-WL 420 nm high-power-LED light source.

The light source was connected with an optical fibre (1000 µm core diameter, *Avantes*) to the cuvette holder over a SMA 905 fibre optic connector. The intensity of the light source was measured to be 18.5 mW / cm$^2$ at the position of the cuvette. The excitation power was measured using a S310C thermal sensor connected to a PM100USB power meter (*Thorlabs*, Germany). The connection piece used to insert the SMA connector into the cuvette holder was replaced by an in-house custom-built connection piece that allows the fibre to be inserted at a distance of 2.0 cm from the cuvette. The detector (AvaSpec-NIR256-1.7TEC, *Avantes*) was set to 0 °C and connected to the cuvette holder with an optical fibre (600 µm core diameter, *Avantes*). Emission spectra were collected at a 90° angle with respect to the excitation beam from 1050 nm to 1500 nm after two measurement runs; every measurement run consisted of five averaged measurements each lasting 9 s. All spectra were recorded using AvaSoft 8.9

(*Avantes*) software and further processed using Microsoft Office Excel (*Microsoft*, USA) and Origin 2018 (*OriginLab*, USA) software.

The singlet oxygen quantum yields ($\boldsymbol{\Phi_\Delta}$) were calculated by comparison with meso-tetrakis(4′-sulphonatophenyl)porphine tetraammonium (**TPPS**), according to equation E1. It was assumed that the $\boldsymbol{\Phi_\Delta}$ of this compound is identical to the one of the analogous tetrasodium salt ($\boldsymbol{\Phi_\Delta}$ = 0.62 in $H_2O$).[5]

$$\text{(E1)} \qquad \boldsymbol{\Phi_{\Delta(x)} = \Phi_{\Delta(std)} \left(\frac{I^{420}_{std}}{I^{420}_{x}}\right)\left(\frac{E_x}{E_{std}}\right)}$$

In E1, the subscript "x" designates the corresponding photosensitizer and "std" the standard (**TPPS**), respectively. "$\boldsymbol{\Phi_\Delta}$" is the singlet oxygen quantum yield. "$I^{420}$" is the rate of light absorption calculated as overlap of the absorption spectrum of either PS or standard and the emission spectrum of the LED light source at 420 nm ($I_0$). The absorption intensity depends exponentially on absorbance A (E2). For A, the measured absorbance values were scaled by a factor of 0.4. *E* is the integrated emission peak of singlet oxygen at around 1270 nm. For these emission spectra, the integrated values were obtained by applying a manual background correction in Origin.

$$\text{(E2)} \qquad \boldsymbol{I^{420} = I_0(1 - 10^{-A})}$$

E1 can be rewritten as:

$$\text{(E3)} \qquad \boldsymbol{\Phi_{\Delta(x)} = \Phi_{\Delta(std)} \left(\frac{S_x}{S_{std}}\right)}$$

In E3, "*S*" designates the slope when "*E*" is plotted against "$I^{420}$" for the two measured concentrations, with a fixed intercept at 0. Errors of the singlet oxygen quantum yields were calculated by error propagation from the standard errors of "$S_x$" and "$S_{std}$".

## 8. $^1O_2$ Luminescence Spectra

### cPt-$H_2$3PyP

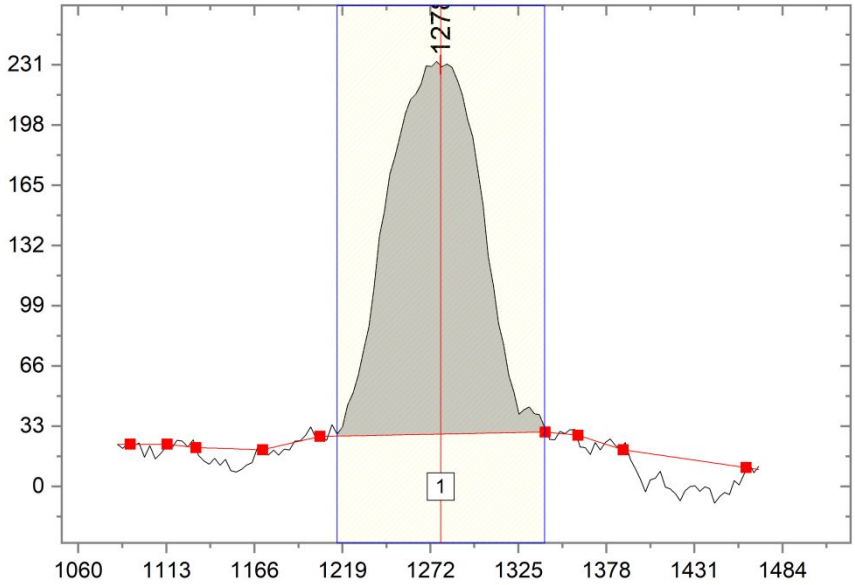


**Figure S19**. Phosphorescence emission spectrum of $^1O_2$ around 1270 nm after $^1O_2$ generation of **cPt-$H_2$3PyP** according to the protocol.

### tPt-$H_2$3PyP

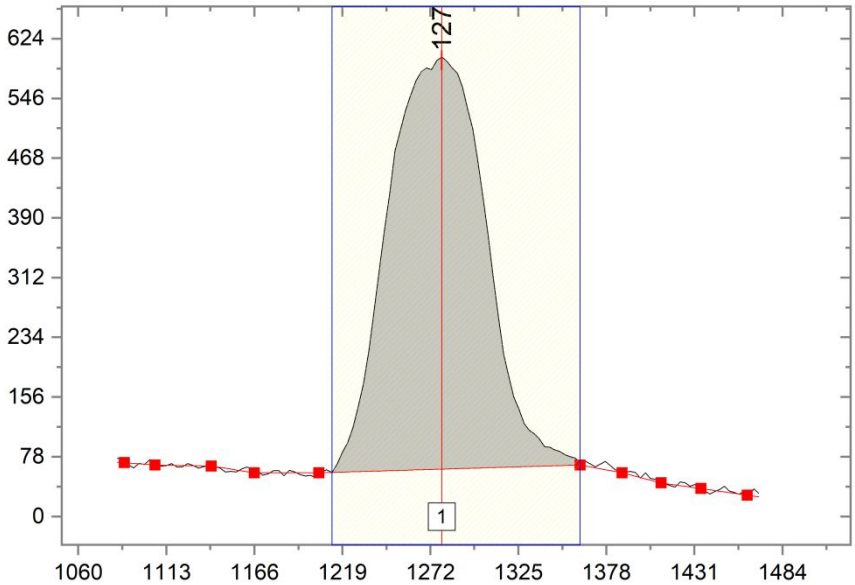


**Figure S20**. Phosphorescence emission spectrum of $^1O_2$ around 1270 nm after $^1O_2$ generation of **tPt-$H_2$3PyP** according to the protocol.

**cPt-Zn3PyP**

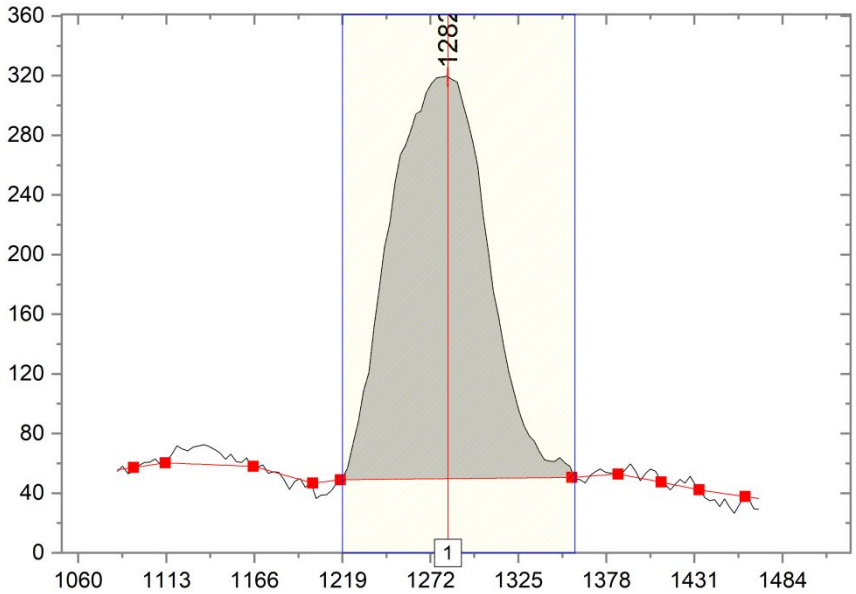


**Figure S21**. Phosphorescence emission spectrum of $^1O_2$ around 1270 nm after $^1O_2$ generation of **cPt-Zn3PyP** according to the protocol.

**tPt-Zn3PyP**

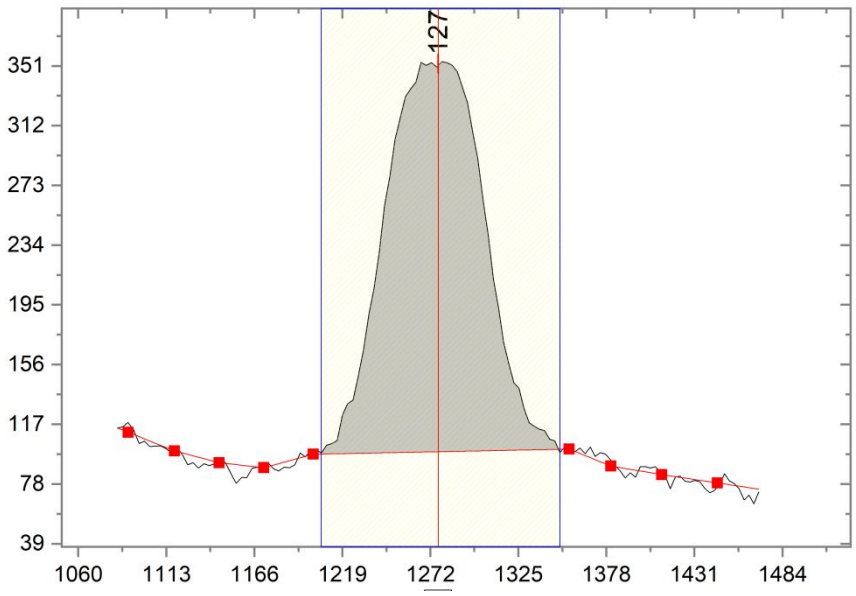


**Figure S22**. Phosphorescence emission spectrum of $^1O_2$ around 1270 nm after $^1O_2$ generation of **tPt-Zn3PyP** according to the protocol.

## 9. Detection of Hydroxyl Radical Production

The fluorescein-derived hydroxyl radical (•OH) sensor 4-aminophenyl fluorescein (APF) was synthesized as described in literature[6] and used as a turn-on sensor to visualize the •OH radicals production by the photosensitizers through the oxidation of the non-fluorescent APF, leading to the fluorescent product fluorescein.[7] A Cary Eclipse fluorescence spectrometer (*Varian*, USA) was used to detect the fluorescence of the emerging fluorescein while using the following settings: excitation at 492 nm, collection of the emission at 525 nm, slit width: 2.5 nm for excitation and emission, averaging time: 1 s. The cuvette was kept at a constant temperature of 25 °C while stirring.

As a positive control, the Fenton's reagent was applied to oxidize the APF. For this purpose, a freshly prepared solution of 5 μM APF (from a stock solution of APF in DMF) and 300 μM ammonium iron(II) sulfate (FAS, from a stock solution of FAS in $H_2O$) in PBS (3 mL total volume) in a cuvette was used as a blank (**Figure S23**) and measured for 30 s to ensure no fluorescence signal is detectable at 525 nm. Then, after 30 s, $H_2O_2$ was added during the measurement in a way that the final $H_2O_2$ concentration reached 300 μM and the solution was measured for another 30 s to visualize the increase in fluorescence, showing the reactivity of the synthesized APF towards the produced •OH radicals (**Figure S23**).

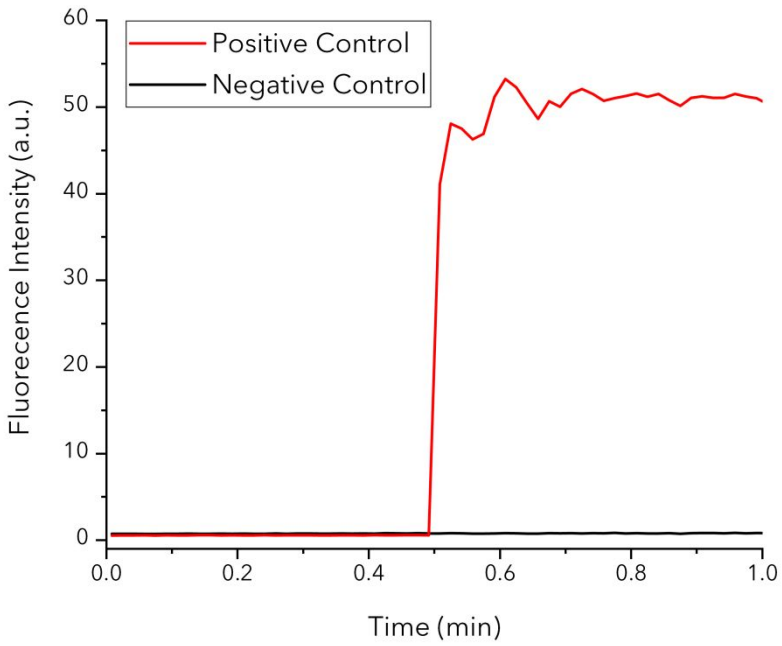


**Figure S23**. Positive and negative control experiments for the APF solution. An increase in fluorescence is detected once the Fenton's reagent produces •OH radicals in the positive control. No increase in fluorescence is detected in the negative control.

To show the generation of •OH radicals by **cPt-$H_2$3PyP**, **tPt-$H_2$3PyP**, **cPt-Zn3PyP** and **tPt-Zn3PyP** upon light irradiation, 1 mM stock solutions of the respective PS in DMF were prepared. Then, 30 μL of each stock solution were 1000-fold diluted with 3 mL of a PBS solution containing 5 μM APF for the experiment. The fluorescence intensity of the solution was measured at 525 nm for 1 min, before the cuvette was irradiated for 30 s with light of 450 nm (See: **Photocytotoxicity Assay**) at a distance of 1 cm from the LED light source while

stirring (light intensity at the distance applied: 11 mW/cm$^2$) and the fluorescence intensity measured again. This process was repeated in 30 s irradiation steps until 5 min of total irradiation time were reached. The mean and the standard deviation of the fluorescence signal for every measurement was determined and plotted.

## 10. Detection of Superoxide Radical Production

The superoxide radical ($O_2^{\bullet-}$) sensor dihydroethidium (DHE) was purchased from Sigma−Aldrich and used as a turn-on sensor to visualize the $O_2^{\bullet-}$ radicals production by the photosensitizers through the oxidation of the non-fluorescent DHE, leading to the fluorescent product ethidium.[8] A Cary Eclipse fluorescence spectrometer (*Varian*, USA) was used to detect the fluorescence of the emerging fluorescein while using the following settings: excitation at 480 nm, collection of the emission at 600 nm, slit width: 2.5 nm for excitation and emission, averaging time: 1 s. The cuvette was kept at a constant temperature of 25 °C while stirring.

To visualize the possible generation of $O_2^{\bullet-}$ radicals by **tPt-Zn3PyP**, **tPt-H$_2$3PyP**, **cPt-Zn3PyP** and **cPt-H$_2$3PyP** upon light irradiation, an experimental setup analogous to the one of the $^{\bullet}$OH radicals detection (**Detection of Hydroxyl Radical Production**) was used. 1 mM stock solutions of the porphyrins in DMF were prepared. Then, 30 µL of each stock solution were 1000-fold diluted with 3 mL of a PBS solution containing 5 µM DHE for the experiment. The fluorescence intensity of the solution was measured at 600 nm for 1 min, before the cuvette was irradiated for 30 s with light of 440 nm at a distance of 1 cm from the LED light source while stirring (light intensity at the distance applied: 11 mW/cm$^2$) and the fluorescence intensity measured again. This process was repeated in 30 s irradiation steps until 5 min of total irradiation time were reached.

None of the four porphyrins **tPt-Zn3PyP**, **tPt-H$_2$3PyP**, **cPt-Zn3PyP** and **cPt-H$_2$3PyP** lead to an increase of the fluorescence signal, indicating that none of the four platinated porphyrins is producing $O_2^{\bullet-}$ radicals under the tested conditions.

As a positive control, potassium superoxide was generated as described in literature.[9] For this purpose, the reaction was downscaled and performed as follows: 0.45 mL of a 6.6 M solution of NaOH were mixed with 0.45 mL of a 30% aqueous $H_2O_2$ solution. Both solutions were at RT. 3 µL of the superoxide solution were added after 2 min to a freshly prepared solution of 5 µM DHE (from a 5 mM stock solution of DHE in DMF) in PBS (3 mL total volume) in a cuvette, so a maximum concentration of 6.7 mM superoxide could theoretically be reached in the cuvette. PBS was used as a blank for the detection of the fluorescence signal at 600 nm. The increase of the fluorescence signal at 600 nm (excitation at 480 nm) emerging from the oxidized DHE is shown below (**Figure S24**).

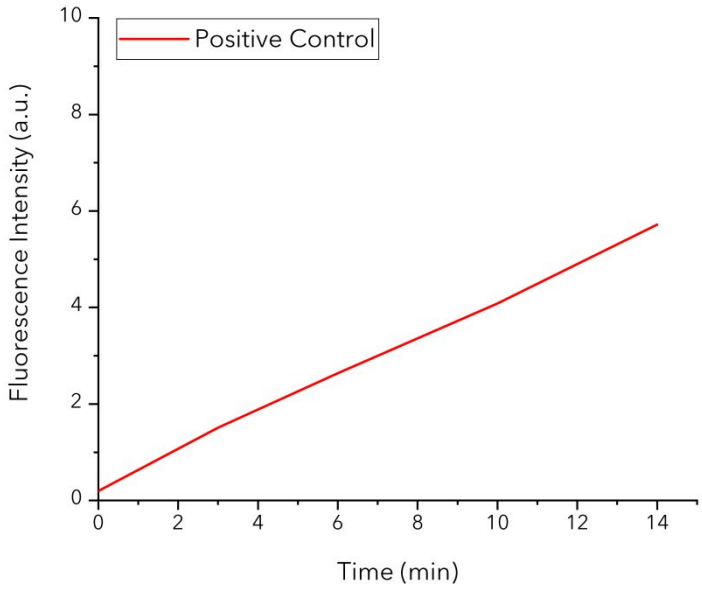


**Figure S24** Positive control experiments for the DHE solution through synthesized potassium superoxide. An increase in fluorescence at 600 nm (excitation at 480 nm) is detected once superoxide radicals are produced in the positive control.

## 11. Photobleaching Assay

The photostabilities of **cPt-H$_2$3PyP**, **tPt-H$_2$3PyP**, **cPt-Zn3PyP** and **tPt-Zn3PyP** have been determined by measuring the corresponding photobleaching quantum yield ($\boldsymbol{\Phi}_\mathbf{d}$) relative to meso-tetrakis(4′-sulphonatophenyl)porphine tetraammonium (**TPPS**).[10] The $\boldsymbol{\Phi}_\mathbf{d}$ is a parameter used to characterise the photostability of a PS and refers to the number of molecules decomposed divided by the number of photons absorbed by the system. The photodecomposition follows first-order kinetics with respect to the irradiation time applied and can be calculated as the ratio of the initial rate of decomposition of PS molecules divided by the initial rate of the number of photons absorbed by using the following equation[10,11]:

$$\text{(E4)} \qquad \boldsymbol{\Phi_d} = \frac{\boldsymbol{\Delta N}}{\boldsymbol{N_{photon}}} = \frac{\boldsymbol{dC \times V \times N_A}}{\boldsymbol{I^{420} \times k \times S \times dt}}$$

Where "*dC*" designates the decrease in concentration over the time period "*dt*", "*V*" is the volume of the solution, "$N_A$" is Avogadro number, "*k*" is the correction constant which characterizes the relation between the measured light irradiance intensity and the real values, "*S*" is the irradiated cell area and "$I^{420}$" is the rate of light absorption calculated as overlap of the 420 nm LED irradiance spectrum and the absorption spectra of the compound that was calculated according to formula (E5):

$$\text{(E5)} \qquad \boldsymbol{I = \int I_{(\lambda)} \times [1 - 10^{-A_{(\lambda)}}] d\lambda}$$

Where $I_{(\lambda)}$ and $A_{(\lambda)}$ are the light-flux intensity of the light source and the absorbance of the compound. The irradiance spectrum of the FC5-LED-WL 420 nm high-power-LED light source (**Figure S18**) was measured with an AvaSpec-ULS2048CL-EVO-RS spectrometer (*Avantes*) using an integration sphere, after calibration of spectrometer according to the standard procedure provided by *Avantes*.

When applying this method relative to **TPPS** as standard, while using the same volume and setup, the $\boldsymbol{\Phi}_\mathbf{d}$ of **cPt-H$_2$3PyP**, **tPt-H$_2$3PyP**, **cPt-Zn3PyP** and **tPt-Zn3PyP** can be calculated by using equation E6:

$$\text{(E6)} \qquad \boldsymbol{\Phi_{d(x)} = \Phi_{d(st)} \times \frac{\frac{dC_x}{dt} \times I_{abs(st)}}{\frac{dC_{st}}{dt} \times I_{abs(x)}}}$$

The values of "*dC/dt*" of the individual compound "*x*" and the standard "*st*" can be derived from the plots of PS concentration vs. irradiation time, which showed the decrease of compound during irradiation. The $\boldsymbol{\Phi}_\mathbf{d}$ of **TPPS** was set to 1 for this relative measurement.

Solutions of **cPt-H$_2$3PyP**, **tPt-H$_2$3PyP**, **cPt-Zn3PyP** and **tPt-Zn3PyP** in DMF were adjusted in quartz cuvettes to absorbance intensities of 1 by using the AvaSpec-ULS2048CL-EVO-RS spectrometer and then irradiated with light (FC5-LED-WL 420 nm high-power-LED) at a constant cuvette temperature of 20 °C and constant stirring at 1200 rpm (see Figure S25). Spectra of every sample measured were recorded continuously by using the program AvaSoft 8 and the activating the "Save Spectra Periodically" option. Initial spectra for every compound were recorded automatically during irradiation for 120 min in intervals of 1 min, then for every compound showing photobleaching as well as the standard the time interval for the decay from absorbance 1.0 to absorbance 0.9 was determined and the automatic measurements were repeated for this time interval in triplicates. For every compound as well as the standard at

least six datapoints were chosen from the automatically recorded spectra and the $\Phi_d$ were then determined by using equation E6.

The $\Phi_d$ of **cPt-H$_2$3PyP**, **tPt-H$_2$3PyP**, **cPt-Zn3PyP** and **tPt-Zn3PyP** measured in DMF relative to **TPPS** were determined to be:

**cPt-H$_2$3PyP**: Photostable for more than 2 h under the measured conditions.

**tPt-H$_2$3PyP**: Photostable for more than 2 h under the measured conditions.

**cPt-Zn3PyP**: 28.5 ± 4.9

**tPt-Zn3PyP**: 44.2 ± 1.6

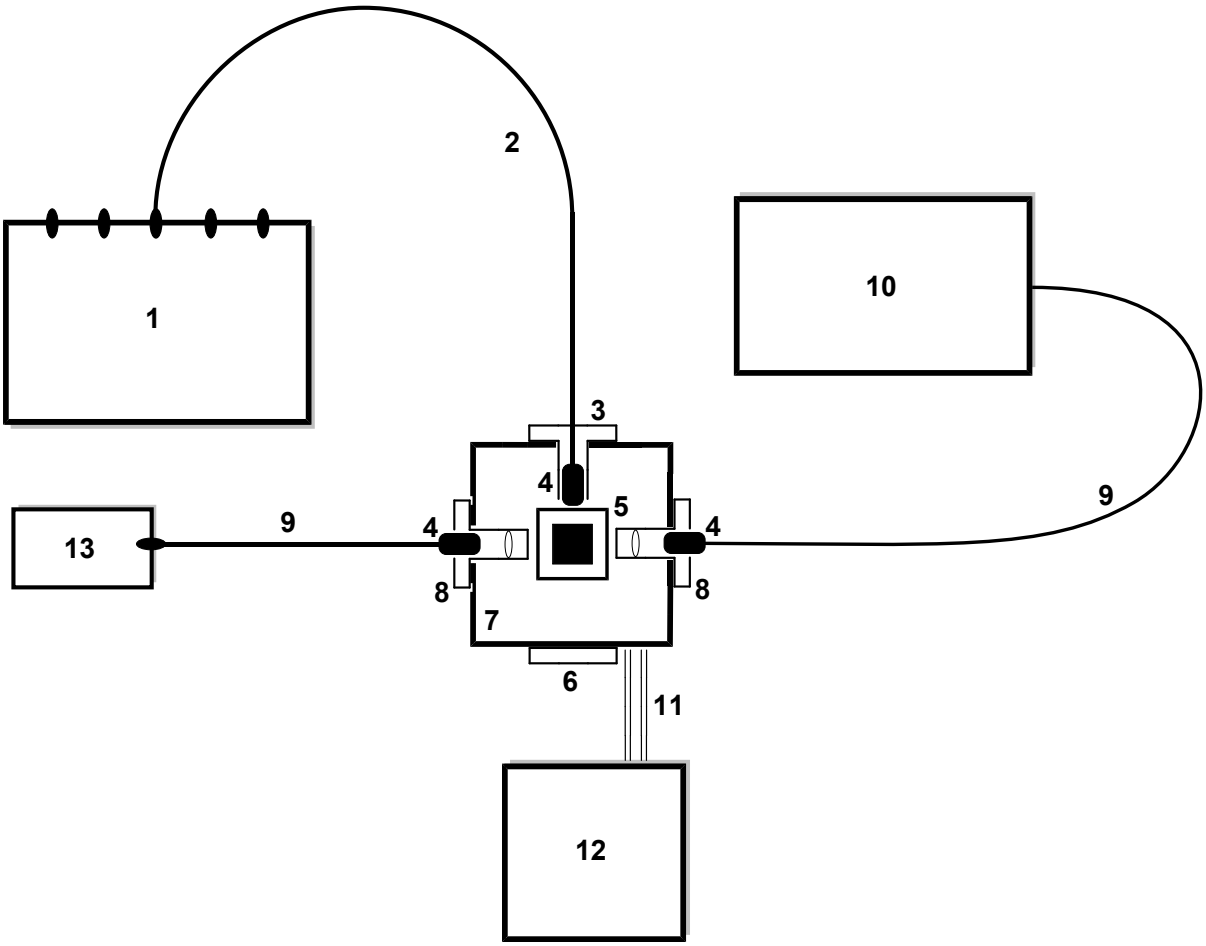


**Figure S25**. Setup used for determination of the photostability. **1)** LED light source, **2)** Optical fibre (1000 μm), **3)** Custom-built connection piece, **4)** SMA 905 fibre optic connector, **5)** Cuvette in cuvette holder, **6)** Blank, **7)** Temperature-controlled Qpod cuvette holder, **8)** Connection piece with QIL-UV AR-coated fused-silica imaging lens, **9)** Optical fibre (600 μm), **10)** Visible light detector, **11)** Plastic hose, **12)** Cooling bath, **13)** Visible light source. Figure modified from Ref. [3] with permission from the European Society for Photobiology, the European Photochemistry Association, and the Royal Society of Chemistry.

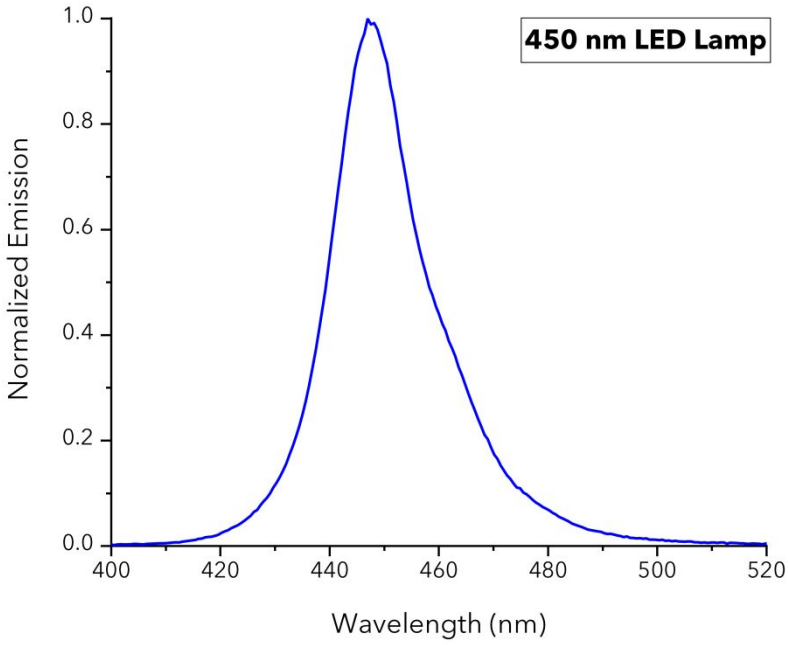


**Figure S26**. Normalized mission spectrum of the 450 nm LST1-01G01-RYL1-00 LED light source.

## 12. References


(1) Mizutani, T.; Horiguchi, T.; Koyama, H.; Uratani, I.; Ogoshi, H. Molecular Recognition and Atropisomerization of [5,10,15,20-Tetrakis(1-pentyl-3-pyridinio)porphyrinato]zinc(II) in Water. *Bull. Chem. Soc. Jpn.* **1998**, *71*, 413.

(2) Choi, E. Y.; DeVries, L. D.; Novotny, R. W.; Hu, C. H.; Choe, W. An Interdigitated Metalloporphyrin Framework: Two-Dimensional Tessellation, Framework Flexibility, and Selective Guest Accommodation. *Cryst. Growth Des.* **2010**, *10*, 171.

(3) Schneider, L.; Larocca, M.; Wu, W.; Babu, V.; Padrutt, R.; Slyshkina, E.; König, C.; Ferrari, S.; Spingler, B. Exocyclically metallated tetrapyridinoporphyrazine as a potential photosensitizer for photodynamic therapy. *Photochem. Photobiol. Sci.* **2019**, *18*, 2792.

(4) Meijer, M. S.; Talens, V. S.; Hilbers, M. F.; Kieltyka, R. E.; Brouwer, A. M.; Natile, M. M.; Bonnet, S. NIR-Light-Driven Generation of Reactive Oxygen Species Using Ru(II)-Decorated Lipid-Encapsulated Upconverting Nanoparticles. *Langmuir* **2019**, *35*, 12079.

(5) Verlhac, J. B.; Gaudemer, A.; Kraljic, I. Water-Soluble Porphyrins and Metalloporphyrins as Photosensitizers in Aerated Aqueous-Solutions. 1. Detection and Determination of Quantum Yield of Formation of Singlet Oxygen. *Nouv. J. Chim.* **1984**, *8*, 401.

(6) Liu, H.-Y.; Zhao, M.; Qiao, Q.-L.; Lang, H.-J.; Xu, J.-Z.; Xu, Z.-C. Fluorescein-derived fluorescent probe for cellular hydrogen sulfide imaging. *Chin. Chem. Lett.* **2014**, *25*, 1060.

(7) Price, M.; Reiners, J. J.; Santiago, A. M.; Kessel, D. Monitoring Singlet Oxygen and Hydroxyl Radical Formation with Fluorescent Probes During Photodynamic Therapy. *Photochem. Photobiol.* **2009**, *85*, 1177.

(8) Pucelik, B.; Paczynski, R.; Dubin, G.; Pereira, M. M.; Arnaut, L. G.; Dabrowski, J. M. Properties of halogenated and sulfonated porphyrins relevant for the selection of photosensitizers in anticancer and antimicrobial therapies. *PLoS One* **2017**, *12*, e0185984.

(9) Stoin, U.; Shames, A. I.; Malka, I.; Bar, I.; Sasson, Y. In situ Generation of Superoxide Anion Radical in Aqueous Medium under Ambient Conditions. *ChemPhysChem* **2013**, *14*, 4158.

(10) Spikes, J. D. Quantum Yields and Kinetics of the Photobleaching of Hematoporphyrin, Photofrin II, Tetra(4-sulfonatophenyl)-porphine and Uroporphyrin. *Photochem. Photobiol.* **1992**, *55*, 797.

(11) Gürol, I.; Durmuş, M.; Ahsen, V.; Nyokong, T. Synthesis, photophysical and photochemical properties of substituted zinc phthalocyanines. *Dalton Trans.* **2007**, 3782.